Astron. & Astrophys. 42, 173–185 (1975)

High Resolution Radio and Optical Observations of NGC 6888

H. J. Wendker and L. F. Smith
Max-Planck-Institut für Radioastronomie

F. P. Israel and H. J. Habing
Sterrewacht Leiden

H. R. Dickel
University of Illinois Observatory

Received March 25, 1975

Summary. NGC 6888 is a filamentary nebulosity associated with the Wolf-Rayet star HD 192163. Maps are presented with a resolution of 5 arcmin at 11 cm and better than 1.5 arcmin at H_α and at 6 cm, 21 cm and 49 cm (continuum). There is a smooth component to the H_α radiation which presumably originates from gas between the filaments. From comparison of the line and continuum intensities, it is found that the smooth component has essentially the same temperature as the filaments. The mechanism by which the filaments are created and maintained is not clear.

Key words: NGC 6888 — nebulosity around WR-stars — galactic radio source

1. Introduction

NGC 6888 (*S* 105) is the nebulosity around the Wolf-Rayet star HD 192163(BD+37°3821). It is one of the nine "ring" nebulae associated with WR stars (Smith, 1968c; Crampton, 1971). Of these, it is the nearest, brightest, and the most regular in shape. It has, besides, a more strongly developed filamentary structure than the other nebulae.

The appearance of the nebula strongly suggests that the ionized gas is distributed in a very thin ellipsoidal shell, roughly but not exactly, centered on the WR star. It was suggested by Johnson and Hogg (1965) that the shape of the nebula is due to material ejected from the WR star at high velocity sweeping up the interstellar medium. Thus, the nebula is of prime interest because of its relationship to the WR stars and to the interaction of material ejected from stars with the interstellar medium.

This paper presents H_α+[N II] isophotes (Section 2.2), 11 cm continuum isophotes obtained with a single dish (Section 3.2), and 6 cm, 21 cm and 49 cm continuum isophotes obtained by aperture synthesis (Section 3.3). The H_α+[N II] and 21 cm observations have resolutions of approximately 30 arcsec; this is adequate to resolve all but the finest structure of the nebula. The single dish (5 arcmin resolution) map is necessary in order to determine the total radio flux density.

2. Optical Observations

2.1. *Previous Optical Data*

The previously known parameters of the star and the nebula are summarized in Table 1. Note that the values given are recomputed for a distance of 1.45 kpc, based on the most recent estimates of M_V, and are not always equal to the values given in the papers quoted.

The optical spectrum of the nebula has been studied by Parker (1964) who observed the brightest filaments in the north and north-western parts. From the [O II] doublet, λλ 3726, 3729, he derived an electron density

Table 1. Data related to HD 192163 and NGC 6888

Star:		
Galactic coordinates	75.5, +2.4	
Spectrum	WN 6	Smith (1968a)
$v(1/\lambda_v=1.94)$	7^m73	Westerlund (1966)
$b-v(1/\lambda_b=2.34)$	+0.25	Smith (1968b)
M_v	−4.8	Crampton (1971), Smith (1972)
$A_v(=1.08\,A_V)$	1.75	Kuhi (1966), Smith and Kuhi (1970)
Distance	1.45 kpc	
Nebula:		
Dimensions	18′ × 12′	
	7.6 × 5.0 pc	
Electron density (in Filaments)	400 cm^{-3}	Parker (1964)

of 400 cm^{-3}. The most unusual feature of the spectrum is the great strength of the [N II] lines near H_α; $I([N\,II])/I(H_\alpha)$ ranges from 0.5 to 2.1 compared to an average value for galactic H II regions of about 0.5 (Johnson, 1953; Dickel *et al.*, 1969). Lozinskaya and Esipov (1968), have also studied the optical spectrum and confirmed the high ratio of $[N\,II]/H_\alpha$. They find an average value of 1.6. Possible explanations will be discussed in Section 5.4.

2. 2. H_α *Plus* [N II] *Isophotes*

NGC 6888 was observed in the calibrated H_α-survey of the Cygnus X-region by Dickel *et al.* (1969). The nebula is shown in Fig. 1. The plate was obtained with the 48 inch Schmidt telescope of the Hale Observatories on flashed Eastman Kodak 103a-E emulsion behind an interference filter with a bandwidth of 80 Å centered on H_α. Figure 6 presents a contour map obtained by microphotometry with a rectangular response pattern having an effective resolution of 38 and 35 arcsec in right ascension and declination respectively. The contours were corrected for a slight decrease of transmission on the filter near the edge of the plate. A linear baseline was fitted between the regions east and west adjacent to NGC 6888 where there is no apparent nebulosity. The main errors of the map resulted from the photoelectric calibration of the plate series (5%), from transferring this from one plate to another (5%) and from the uncertainty of the baseline level (5%). The resulting rms-error is ≦15%.

Three bright stars within the boundary of the nebula, the central star, HD 192163, and two foreground stars, are marked by asterisks in Fig. 6. Their flux was subtracted by hand from the total integrated flux contained in the map. The final flux of the nebula is:

$$S(H_\alpha+[N\,II])=1.1\times10^{-12}\ W\,m^{-2}.$$

In order to obtain the flux due to H_α alone, we must correct for the contribution due to the [N II] lines which are included in the filter bandpass. The intensity ratio, $[N\,II]/H_\alpha$, is not constant over the nebula. Figure 7 combines the tabular data of Parker (1964) Losinskaya and Episov (1968) and Losinskaya (1970) to divide the nebula into regions of approximately constant intensity ratio $[N\,II]/H_\alpha$. The numbers give the factor $I(H_\alpha)/$

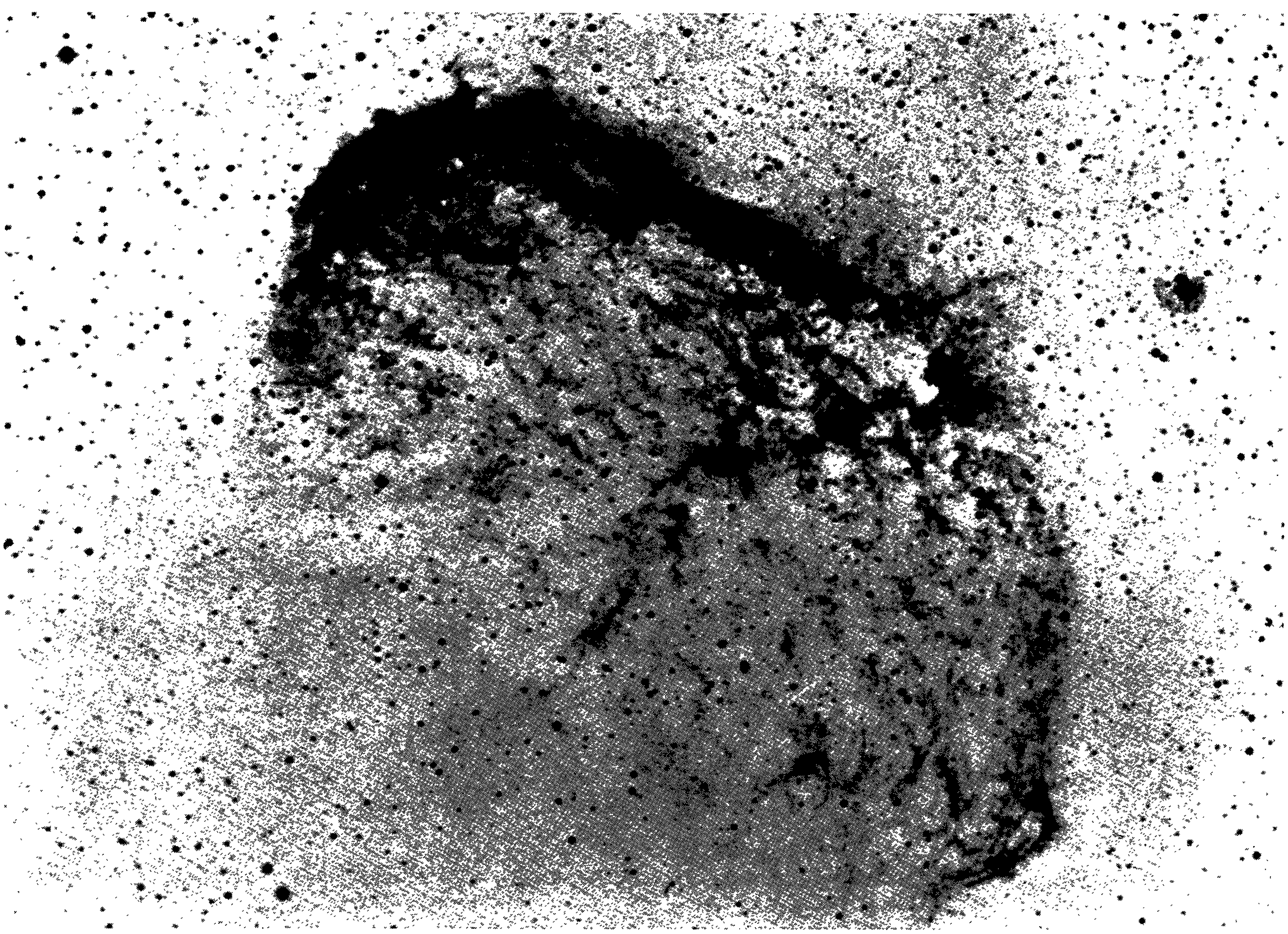

Fig. 1. Photograph of NGC 6888 in H_α+[N II]. See Text. Taken with the Hale Observatories 48" Schmidt-telescope

$I(H_\alpha+[N\,II])$. The integrated H_α flux obtained by combining Figs. 6 and 7 is

$$S(H_\alpha) \approx 0.55 \times 10^{-12}\ \mathrm{W\,m^{-2}}.$$

There are several structural features which we wish to point out:

1) The faint ridge (at about $\alpha=20^h11^m$, $\delta=38°12'$) extending from the northeast corner of NGC 6888 towards the south is real and visible as a faint patch on the original plate. It can also be seen on the Palomar Atlas Sky Survey prints and does not appear to be physically related to NGC 6888. (This impression is confirmed by reddening determinations: see Section 4.3.) Its total flux, uncorrected for [N II], is 6×10^{-14} W m^{-2}.

2) The distribution of radiation is very asymmetric. About 35% of the total radiation originates from the brightest group of filaments at the northeastern end; the bright group on the northwestern side contributes 25% and the group at the southwestern end 15%. Thus, 75% of the radiation comes from only 25% of the area of the nebula.

3) The sharpness of the boundaries of the ring is not uniform. On the northeastern and southwestern ends (around $\alpha=20^h10^m45^s$, $\delta=38°18'$ and $\alpha=20^h09^m50^s$, $\delta=38°04'$) the boundary is sharper than on the northwestern side. This can be seen on the photograph (Fig. 1) and also on the isophotes (Fig. 6). Tracings were made with 2 arcsec resolution perpendicular to the boundary at several points. It was found that on the northeastern and southwestern ends the rise from minimum to maximum intensity takes place in about 13 ± 3 arcsec; this corresponds to a linear distance of about 0.1 pc. On the northwest side the rise is about half as fast, taking place over about 0.25 pc.

On the southeast side of the nebula, the intensity decreases slowly and it is difficult to determine the boundary. We will assume, in what follows, that it may be represented by the completion of the ellipse defined by the brighter edges.

4) One particular feature of the shell boundary has been previously overlooked. Faint filaments protrude from the northwest side of the nebula beyond the well-defined rim. This feature is hardly visible on the Sky Survey prints, but can clearly be seen on the photo-

Fig. 2. Radiophotograph of the 1415 MHz observations of NGC 6888

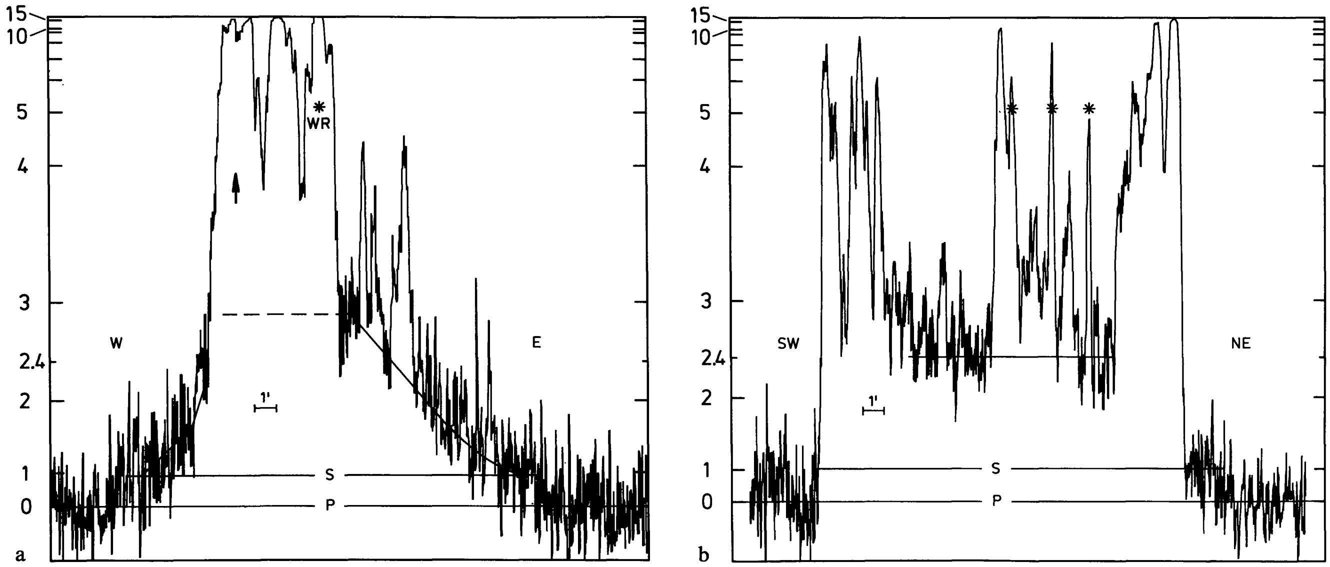

Fig. 3a and b. Microphotometer scans along the lines indicated in Fig. 6 with a resolution of 3 arcsec

graph in Fig. 1. These small filaments stand in marked contrast to the majority of the filaments in the nebula which appear to be oriented tangentially within an ellipsoidal shell.

2.3. H_α *Observations of the Smooth Component*

A strongly exposed plate of NGC 6888 in H_α only was obtained in conjunction with R. Louise using the "reducteur focal" (Courtès, 1973) on the 120 cm telescope of Haute Provence Observatory. The filter had a bandpass of 10 Å in parallel light; its properties in the $F/6$ beam of the telescope are not known, but the transmission of the [N II]-lines is certainly greatly reduced.

Figure 3a and b show tracings across the nebula along the lines A and B maked in Fig. 6. These were made with a projected slit, equivalent to 3.3 arcsec square on the plate. The clear plate (P) and the sky background (S) (due to moonlight) are marked. It is obvious that underlying the filaments is a component of the radiation which is smooth on a scale of 10 arcsec and has a distribution similar to that of the filaments, in the sense of being most intense in the northwestern half of the nebula and decreasing smoothly to the southeast. Comparison of Fig. 3b with the H_α+[N II] contour map, Fig. 6, shows that the smooth background on this trace corresponds to isophote "75". The smooth background is clearly somewhat stronger further to the northwest, where the strongest filaments are found (see trace A); however, the level of the smooth component in trace B is clearly defined and the corresponding levels on the contour maps are easily defined; thus, we adopt this level as representative of the smooth component.

3. Radio Observations

3.1. *Previous Radio Observations*

All previous observations were made with single dish instruments and did not have, in general, sufficient resolution to detect structure. Thus, only integrated flux density values are available. The data are summarized in Fig. 4 which clearly shows that the radio radiation of the complex is in first approximation of thermal origin and is optically thin. The value for the flux at 318 MHz includes a correction for the dimensions of the source, from that of the optical nebula (as assumed by Terzian, 1970) to 18 by 15 arcmin as indicated by the isophotes of Felli and Churchwell (1972). The radio source extends to the south and southeast of NGC 6888 covering the position of the faint patches of nebulosity which were mentioned in the previous section, and which are not necessarily physically related to NGC 6888. It follows that not all the observed integrated flux can be attributed to NGC 6888.

3.2. *Single Dish Observations at 11* cm

In order to obtain a more accurate total flux density for NGC 6888, alone, the region was mapped with the 100 m telescope of the MPIfR at Effelsberg at 2695 MHz. At this frequency, the beam has a half-power total width of 4.8 arcmin. Six or more scans at each position were averaged, resulting in an rms noise of 0.02 K T_b or better. The zero level of the map was set equal to that defined (Wendker, 1970) for the Cygnus X region which is just north of NGC 6888 and into which several long scans were extended. The remainder were tied together by a number of cross scans.

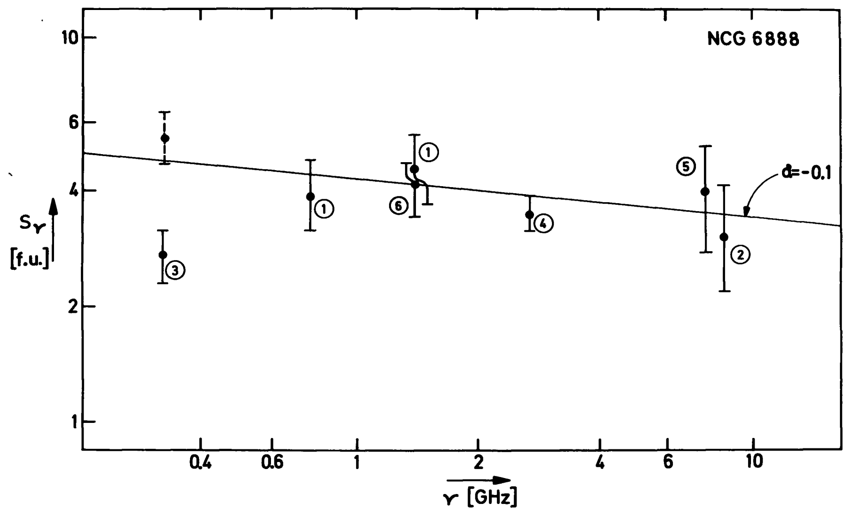

Fig. 4. Radio spectrum of NGC 6888 from low resolution single dish observations. The solid line representing a spectral index of −0.1 is estimated by eye. The references are: (1) Johnson and Hogg (1965), (2) Lozinskaya (1970), (3) Terzian (1970), (4) Schwartz (1968), (5) Johnson (1971), (6) Felli and Churchwell (1972)

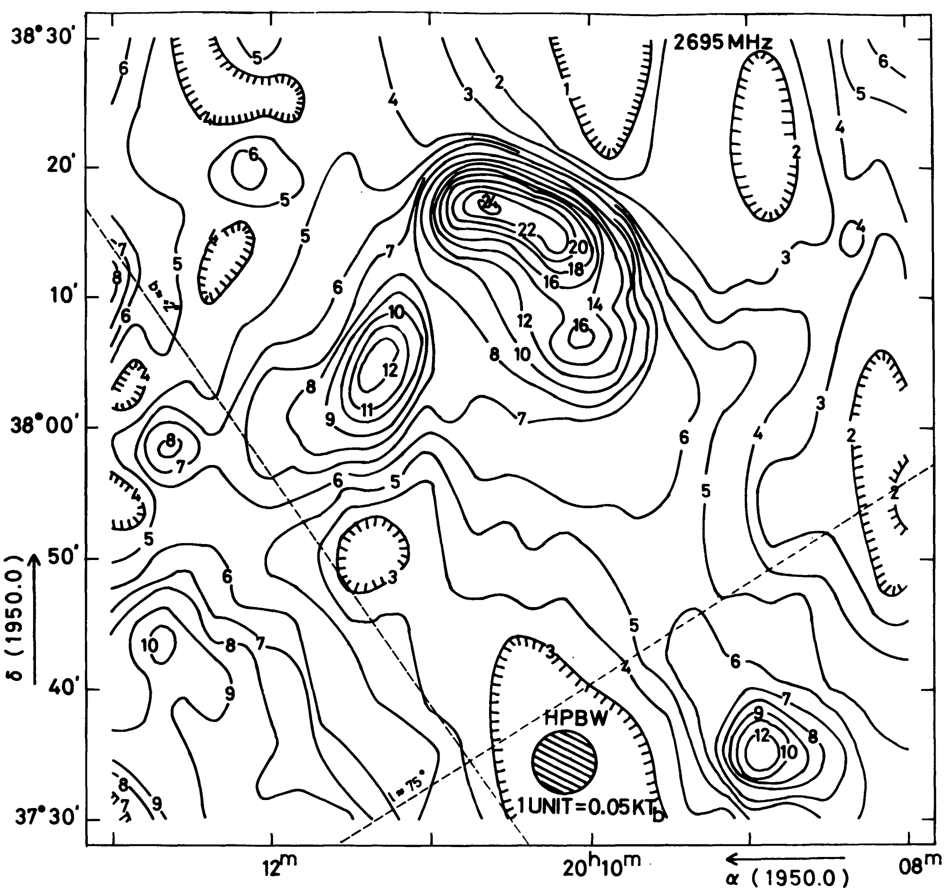

Fig. 5. Contour map of NGC 6888 and surrounding area at 2695 MHz

In the 11 cm map (Fig. 5) the main source, NGC 6888, and a second source, corresponding to the faint ridge, are clearly resolved. There is also a weak and very extended component, best visible to the south of NGC 6888, which is probably unrelated to the two smaller sources. Its main effect is to cause the background level to decrease from south to north across the region of NGC 6888.

The brightness temperature isophotes of NGC 6888 were planimetered to obtain the total flux density. In

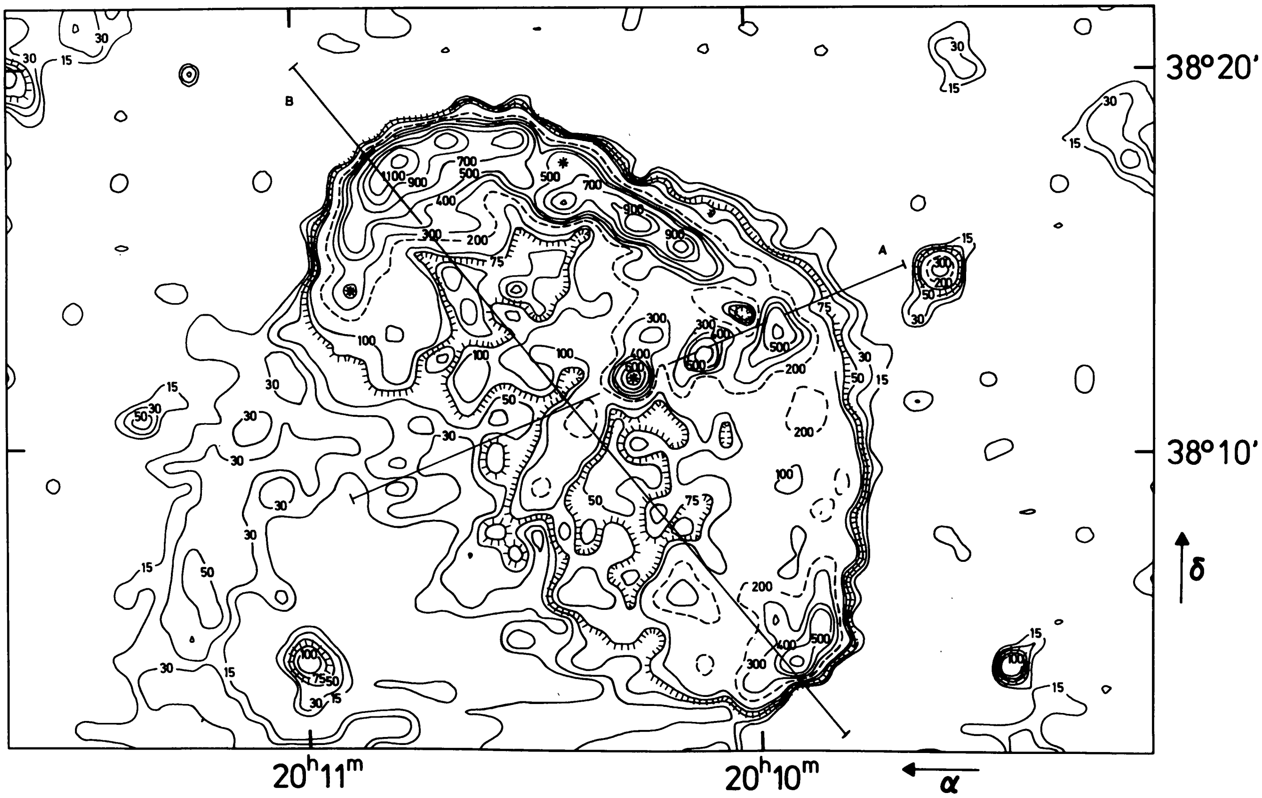

Fig. 6. Contour map of the H_α+[N II] intensities of NGC 6888 from the plate shown in Fig. 1. 1 contour unit $=3.74\times10^{-10}$ W m^{-2}sterad^{-1}

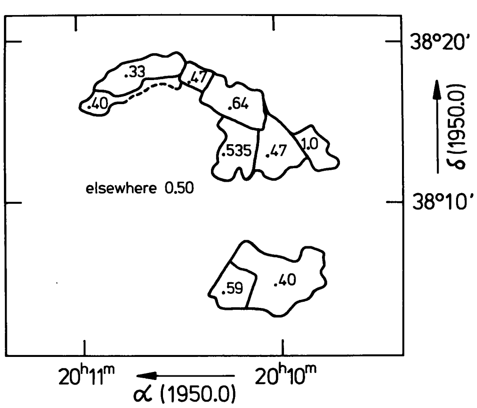

Fig. 7. Map representation of the correction factor to be applied to the contour map of Fig. 6 when converting from H_α+[N II] intensity to H_α intensity alone. See text

the north and west the boundary is obvious; in the south and east the contour level labelled "8" was taken as the boundary. The extended component was estimated to contribute 0.2±0.1 K over the area of NGC 6888. This correction is uncertain and represents the largest source of error in the flux determination. The result is

$$S_{2695}=2.5\pm0.3\times10^{-26}\ \mathrm{W\,m^{-2}\,Hz^{-1}}.$$

To compare with the higher resolution maps to be presented in Section 3.3, NGC 6888 was divided into four components which were represented by gaussians: two for the northern filaments, one for the southern maximum and one for the underlying large component. The background was treated as one component centered slightly south of NGC 6888. The rms-value of the model fit was only slightly larger than the observational noise. The derived values of the integrated flux density of the various components are given in Table 3. The total flux density of 2.6×10^{-26} W m^{-2} Hz^{-1} for NGC 6888 is in excellent agreement with the value derived by integration of the isophotes.

The source to the southeast of NGC 6888 can be approximated by a gaussian of peak intensity 0.44 K T_b (above an estimated zerolevel of 0.20 K) with half-width of 13×8 arcmin corresponding to a flux density of 0.9×10^{-26} W m^{-2} Hz^{-1}.

3.3. Aperture Synthesis Observations at 49, 21 and 6 cm

To obtain higher resolution radio observations of NGC 6888, we used the Westerbork Synthesis Radio Telescope. This instrument consists of an array of ten fixed and two mobile 25 m dishes, forming twenty simultaneous interferometers. The instrument is described in detail by Baars and Hooghoudt (1974); the 21 cm receiving system is described by Casse and Muller (1974). Parameters relevant to the telescope and our observations are given in Table 2. We used the standard calibration and reduction procedures, de-

Table 2. Parameters for WSRT observations

Frequency [MHz]	4995	1415	609.8
HPBW Primary beam [arcmin]	12	37.6	83
HPBW Synthesized Beam [arcsec]	7×11	25×39	58×88
R.M.S. Noise [mJy]	0.6	0.6	2.0
Field Center	$20^h10^m40.8^s$ 38°16′12″	$20^h10^m16.8^s$ 38°12′36″	$20^h10^m21.0^s$ 38°12′00″
Observ. Time	4×12^h	4×12^h	2×12^h
Observ. Dates	Nov 1972 Dec 1972 Jan 1973 May 1973	Apr 1971 May 1971 Jun 1971	Aug 1973 Sep 1973
Spacings Interferometer [m]	36–1458	36–1458	54–1458
Increment [m]	18	18	36

scribed by Högbom and Brouw (1974) and van Someren Gréve (1974). The observations are represented by maps with contours of constant flux-density per beam, i.e. constant brightness temperature (Figs. 8—10). In the maps, the contours are labelled in units of 3.75 K (corresponding to 5 m.f.u. per synthesized beam). The 21 cm radiograph presented in Fig. 2 was made using an interactive program and a PDP 9 computer at Groningen University (Ekers *et al.*, 1973). The following comments are in order.

1) In all maps interferometer spacings shorter than 36 m are missing. As a consequence, extended structures are inadequately observed. About 50% of the flux-density is missing for components larger than 4 arcmin at 6 cm, larger than 12 arcmin at 21 cm, and larger than 30 arcmin at 49 cm. Given the dimensions of NGC 6888, this means that the source is completely detected at 49 cm, that one expects about 50% of the smooth component to be missing at 21 cm, and that only the bright filaments can be observed at 6 cm.

2) The lack of a zerospacing and (in the case of the 6 cm and 21 cm observations) also the lack of the 18 m spacing implies a slight depression of the true zerolevel. Only in the case of the 49 cm observation is the (u, v) plane regularly sampled, so that this zerolevel depression is linear. The magnitude of the zerolevel depression can be estimated from crosscuts.

3) Flux densities were determined by planimetering the contourmaps. The results are listed in Table 3. The 21 cm flux-densities were derived from a map smoothed to a 2 arcmin synthesized beamsize in order to increase the signal-to-noise ratio for the extended structure. The flux-densities of the extended component of NGC 6888, as observed at both 11 cm and 49 cm is consistent with the notion that at 21 cm 0.6×10^{-26} W m^{-2} Hz^{-1} is missing out of a total of 2.6×10^{-26} W m^{-2} Hz^{-1}. A missing flux-density of 40% is indeed the amount expected for structure on a scale of 10 arcmin.

From Table 3 it appears that all components of NGC 6888 are thermal in nature and optically thin. Finally we have a possible detection (three times the r.m.s. noise) of the WR star itself; upper limits are given for the other two observed wavelengths.

4. Comparison of Radio and Optical Intensities

4.1. General Features

The resemblance between the H_α+[N II] photograph (Fig. 1) and the 21 cm radiograph (Fig. 2) is striking. However, comparison of Figs. 6 and 9 shows that the isophotes are not identical: The peaks in the northeast

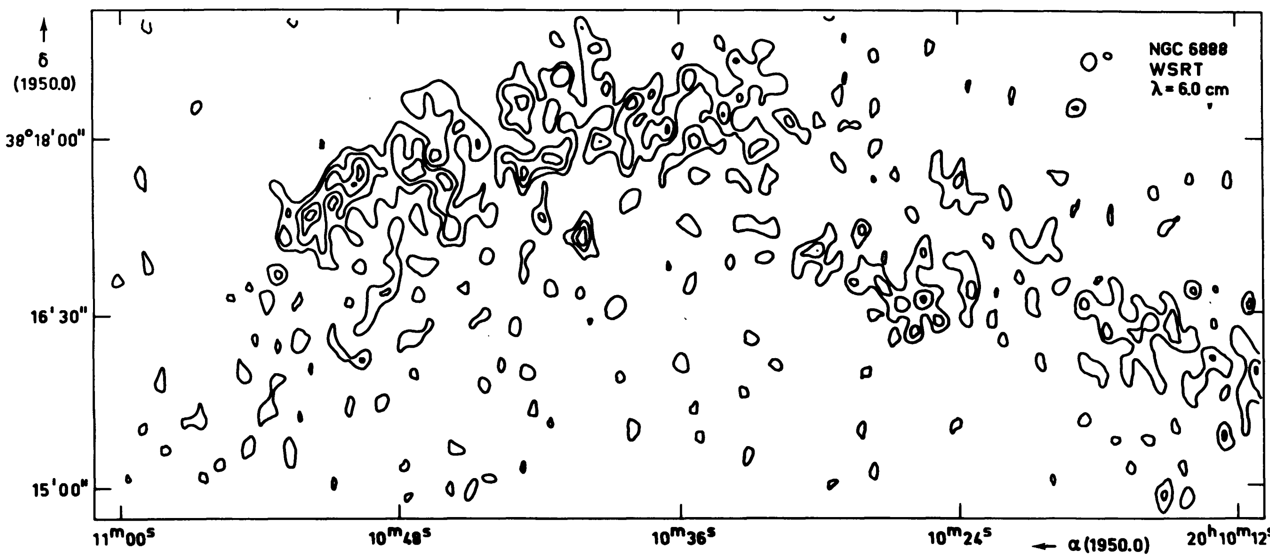

Fig. 8. Contour map of the 6 cm observations with the Westerbork Synthesis Radio Telescope. 1 contour unit = 3.75 K $T_b = 2.0\times10^{-20}$W m^{-2}Hz^{-1}sterad^{-1}. Drawn contours are: 0.15 to 0.6 in steps of 0.15

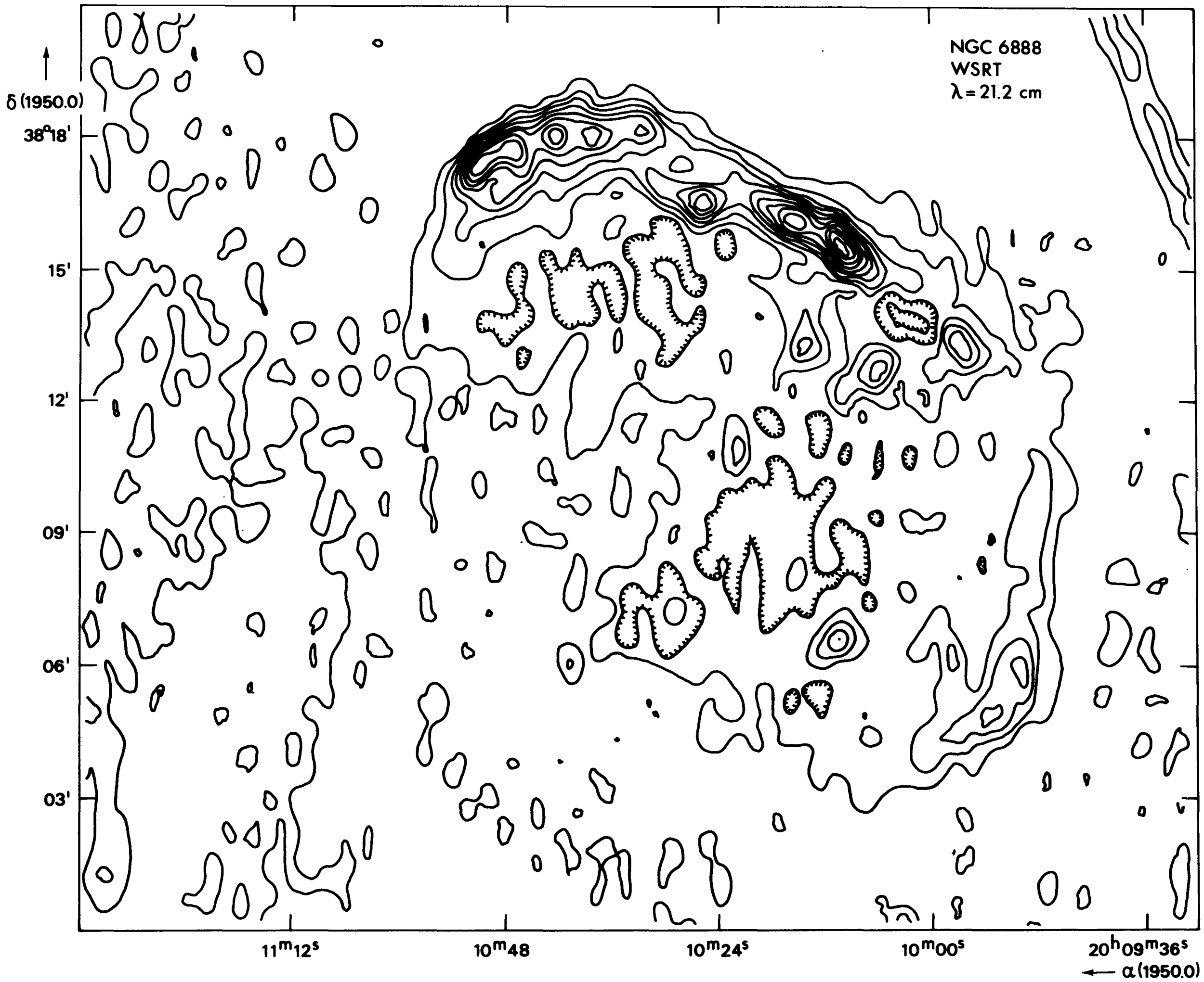

Fig. 9. Contour map of the 21 cm continuum observations with the Westerbork Synthesis Radio Telescope. 1 contour unit = 3.75 K $T_b = 1.4 \times 10^{-21}$ W m^{-2}Hz^{-1}sterad^{-1}. Drawn contours are: 0 (dashed), 0.5 to 5.0 in steps of 0.5

do not coincide in shape or position and the ratios of peak intensities (line/continuum) vary by a factor 1.5 from peak to peak, which is not due to beam smearing because the resolution is the same at both wavelengths. This is probably due to variable contributions of [N II] to the intensity. After correction for [N II] according to Fig. 7, the peak-to-peak variation remains, which is no surprise, since the H_α/[N II] ratio is probably variable on a smaller scale than the data permit to determine. There is, however, no systematic effect, such as might result from uneven foreground absorption.

4.2. The Temperature of the Gas in the Smooth Component

We suppose that the smooth H_α component (Section 2.3) comes from gas between the filaments and is also confined to a shell (rather than filling the volume of the ellipsoid).

The H_α emission coefficient $\varepsilon(H_\alpha)$ is given by Pengelly (1964) as a function of temperature. In the range 10^4 to 10^5 K, we have, to good accuracy:

$$4\pi I(H_\alpha) = 4\pi \int \varepsilon(H_\alpha) dl \approx 3.53 \times 10^{-24} \int N_e^2 T_e^{-1} dl [\mathrm{W\,m^{-2}}]. \quad (1)$$

Thus, the difference in surface brightness between a filament and the interfilament region reflects a difference in the density (N_e), temperature (T_e), path length (l), or all three.

We may test directly for a difference in temperature by considering the corresponding relation for emission of free-free radio radiation. From the emission coefficient, ε_ν, given by Oster (1961) and the approximation formula given by Altenhoff *et al.* (1961), we derive:

$$4\pi I_\nu = 4\pi \int \varepsilon_\nu dl = 8.17 \times 10^{-40} \int N_e^2 T_e^{-0.35} \nu^{-0.1} dl [\mathrm{W\,m^{-2}}]. \quad (2)$$

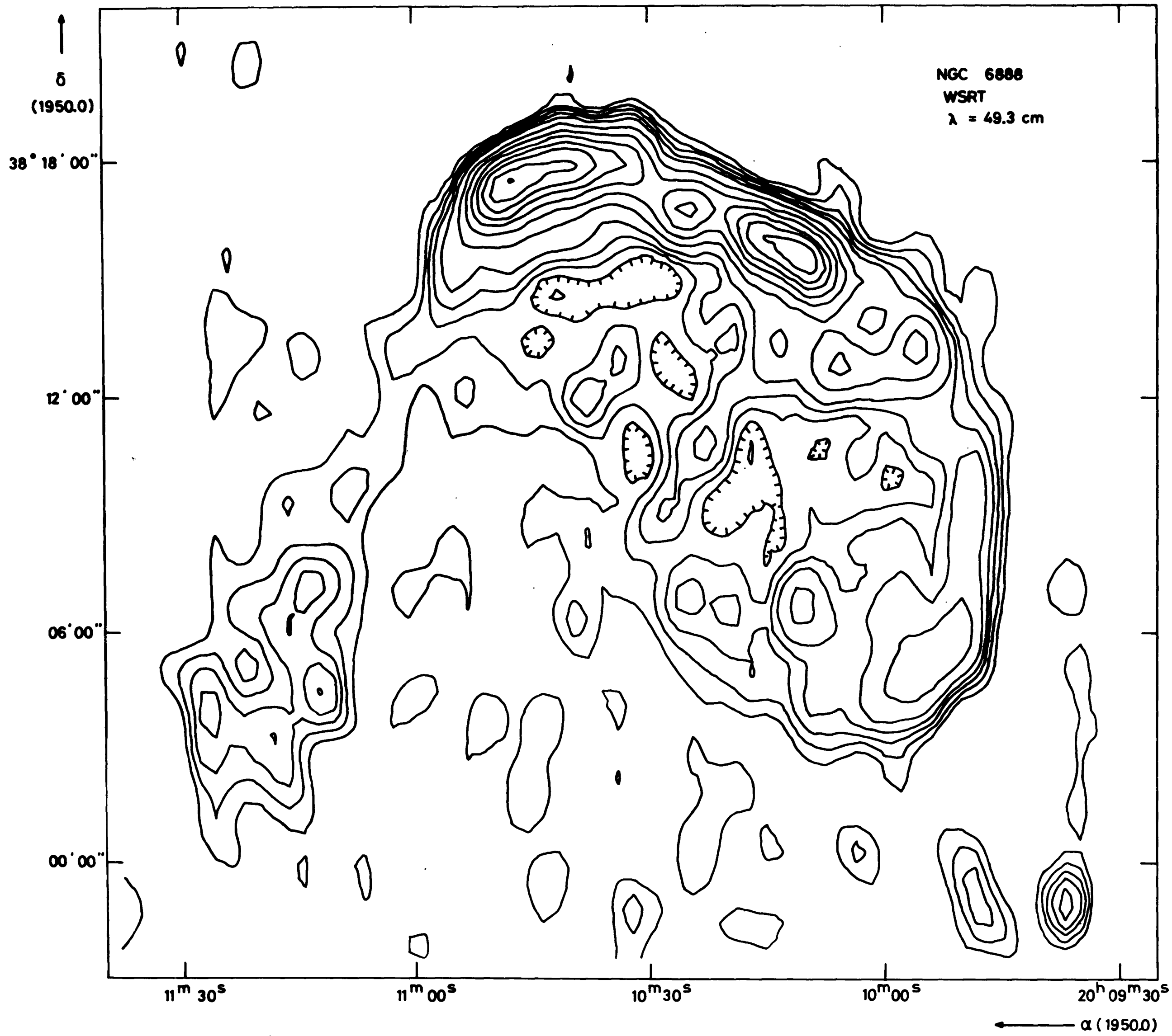

Fig. 10. Contour map of the 49 cm observations with the Westerbork Synthesis Radio Telescope. 1 contour unit = 3.75 K $T_b = 2.7 \times 10^{-22}$ W m^{-2} Hz^{-1} $sterad^{-1}$. Drawn contours are: 0.75 to 3.0 in steps of 0.75 and 4 to 18 in steps of 2

Table 3. Flux densities (10^{-26} W m^{-2} Hz^{-1})

	Wbk (Fig. 8)	Eff (Fig. 5)	Wbk (Fig. 9)	Wbk (Fig. 10)
Wavelength [cm]	6	11	21	49
Northern Filaments	0.6 ± 0.2	0.9 ± 0.2	0.8 ± 0.1	0.8 ± 0.1
Large Component	—	1.6	0.8 ± 0.1	1.55 ± 0.2
Total NGC 6888	—	2.6 ± 0.3	2.05 ± 0.3	2.75 ± 0.4
SE Ridge Source	—	0.9 ± 0.1	0.3 ± 0.1	0.27 ± 0.04
HD 192163	0.0035 ± 0.0015	—	< 0.0015	< 0.0025

We define a "contrast" R by:

$$R = I(\text{filament})/I(\text{smooth}). \quad (3)$$

It may then be shown that:

$$R(\mathrm{H}_\alpha)/R(\mathrm{ff}) = [T_e(\text{smooth})/T_e(\text{filaments})]^{0.65}. \quad (4)$$

Thus, if the temperature of the gas in the smooth component is significantly different from that in the filaments, the observable quantity on the left hand side will differ from unity.

To determine the two values of R, we use the group filaments northwest of the WR star (marked by an arrow in Fig. 3a). This group has the desirable properties: that the filaments are close enough together over a large enough area, that the smoothing due to resolution of the 21 cm observations (24 × 39 arcsec) and of the H_α+[N II] observations (38 × 35 arcsec) should have no effect on the peak intensity; that the filaments do not appear to overlap and the peak intensity is not much greater than that of bright single filaments (see Fig. 3a).

A representative value for the brightness of the smooth background in H_α+[N II] was established (Section 2.3) to be equivalent to contour "75" in Fig. 6. Thus, the H_α+[N II] contrast ratio is 700/75=9.3. The correction factor for [N II] is not known: the factor in the filaments is 0.53 (Fig. 7); however, the degree of ionization of nitrogen is probably higher in the interfilament region than in the filaments, [N II] thereby relatively weak, and hence most of the radiation in the smooth component may be H_α. Thus, the contrast is expected to be less for H_α alone than for H_α+[N II]. We may set limits $5 < R(H_\alpha) < 9.3$.

The H_α tracing, Fig. 3a, passes through the relevant group of filaments. They are unfortunately overexposed; one can only say with certainty that $R(H_\alpha)$ is greater than $10/1.4 \approx 7$ and is probably less than $15/1.4 \approx 11$. Thus, our best estimate from available data is $R(H_\alpha) = 8 \pm 2$.

To determine R(ff), we must first determine the equivalent level of the smooth component. We note first that the so-called "large component" for which fluxes were derived and listed in Table 3, obviously includes some weak filaments which we wish to avoid and therefore proceed as follows: We note that the "75" isophote in the H_α+[N II] map is nearly coincident with the "zero" isophote on the 21 cm map. Zero point depression in this map is 0.75 K T_b. In addition, distributing the missing flux of $0.6 \pm 0.3 \times 10^{-26}$ W m^{-2} Hz^{-1} (see Section 3.3) evenly over the optical extent of the nebula (18 × 12 arcmin = 1.44 10^{-5} sterad), we find a contribution of again 0.75 K T_b. Thus, we derive I(ff) = 1.5 K T_b for the smooth component. The peak brightness of the relevant group of filaments in our 21 cm map is 8.25 K T_b. Thus, $R(\text{ff}) = (8.25 + 1.5)/1.5 = 6.5 \pm 2$.

Thus, $R(H_\alpha)/R(\text{ff}) = 1.2 \pm 0.3$ and we conclude that the gas responsible for the smooth component probably has the same temperature as the gas in the filaments. Whether the smooth component is due to interfilament gas or to a blending of numerous small, weak filaments cannot be established from the present data.

4.3. *Temperature and Reddening of the Nebula*

Combining Eqs. (1) and (2), allowing for interstellar absorption of H_α, and integrating over the source, we obtain:

$$S_\nu/S(H_\alpha) = 2.31 \times 10^{-16} T_e^{+0.65} \nu^{-0.1} 10^C \qquad (5)$$

where C is the logarithmic absorption at $H_\alpha = 0.4 A(H_\alpha) = 0.31 A_V$, where $A(H_\alpha)$ and A_V are the absorption, in magnitudes, at the wavelength of H_α and V, respectively.

From Section 3.3, the total flux density at 21 cm is $(2.65 \pm 0.3) \times 10^{-26}$ W m^{-2} Hz^{-1}. From Section 2.2, the total H_α flux is $(0.55 \pm 0.1) \times 10^{-12}$ W m^{-2} (where the possible error does not allow for an error in the correction for [N II]). Expressing T_e in units of 10^4 K, we have:

$$T_e^{+0.65} 10^C = 4.3 \pm 0.8 .$$

If the absorption over the whole nebula is equal to that for the star, i.e. $A_V = 1.62$ mag, then $T_e = 16000 \pm 6000$ K. Alternatively, if we assume $T_e = 10^4$ K, then $A_V = 2.05$ mag. An error of 0.4 magnitudes in the visual absorption of the star is unlikely. Large variations of foreground absorption are unlikely (see Section 4.1). Thus, the temperature of the nebula might be higher than average for galactic nebulae; it is also possible that we have underestimated the H_α flux by overestimating the correction for [N II] (see Section 2.2).

Applying Eq. (5) to the emission from the southeast-ridge-source, which we found to have an 11 cm flux-density of 0.9×10^{-26} W m^{-2} Hz^{-1} and an H_α flux of 6×10^{-14} W m^{-2}, we find that either $T_e > 10^5$ K or $A_V > 3.7$ mag. The required temperature might be reduced by a factor of 3 if [N II] were very strong; however, the value would still be unlikely and we conclude that the absorption of this source is rather higher than that for NGC 6888 and it is likely that this nebulosity is at a greater distance than, and is unassociated with NGC 6888, as already assumed.

5. Discussion

5.1. *On Dynamical Models for the Relation between Nebula and Star*

Johnson and Hogg (1965) used a simple, spherically symmetric model, based on conservation of momentum, to argue that NGC 6888 (and other such nebulae around WR stars) are expanding shells swept up by a strong stellar wind from the central star. A more elaborate model, that also considers the structure of the shell has been developed by Pikel'ner (Pikel'ner, 1968; Pikel'ner and Shcheglov, 1969) and applied to NGC 6888 by Avedisova (1972), Pikel'ner's model predicts that the swept up interstellar mass forms a thin skin around a thick, very hot (10^8 K) shell of shocked stellar wind gas. It is, in fact, the gas pressure in this thick hot shell that pushes the observed cool shell outwards, sweeping up more gas from the surrounding medium. The observed shell is bounded on the outside by an ionization shock. As gas passes through the shock, it is heated to temperatures of about 10^6 K, but is cools relatively quickly to a temperature in equilibrium with the stellar radiation field, i.e. 10–15000 K. The observations described in this paper refer to the "cool" layer of gas that borders on the thick, hot, shocked stellar wind shell.

We consider in the following sections: the mass and thickness of the shell (Section 5.2); the origin of the material in the shell (Section 5.3); the [N II]/H_α ratio (Section 5.4); the nature of the filaments (Section 5.5); and HD 192163 as a radio star (Section 5.6).

5.2. *Mass and Thickness of the Shell*

Using the formulae given by Smith and Batchelor (1970) together with the newly derived total flux for NGC 6888 ($2.65 \pm 0.3 \times 10^{-26}$ W m^{-2} Hz^{-1} at 21 cm), an assumed density throughout of 400 cm^{-3} (Parker, 1964) and a distance of 1.45 kpc (Table 1), the mass and radiating volume are 4.6 $M_\odot$ and 0.36 pc^3, respectively for $T_e = 10^4$K and 5.3 $M_\odot$ and 0.41 pc for $T_e = 1.5 \times 10^4$K. The mean shell thickness is 0.01 pc, corresponding to 1.4 arcsec. If the filaments are cylindrical and cover 1/4 of the surface, their thickness should be of order 6 arcsec, in reasonable agreement with the observed size of the stronger filaments. The ratio of the mean shell thickness to the distance from the star ($\sim$3 pc) is of order 3×10^{-3}, to be compared with the theoretically predicted upper limit of 5×10^{-2} (Pikel'ner, 1968).

Revision downwards (by 40%) of the mass of the nebula will reduce (by the same factor) the estimates of the rate of mass loss from the star (Georgelin and Monnet, 1970; Avedisova, 1972). However, a factor of 2 is probably insignificant compared to other uncertainties in this quality.

5.3. *Evolution of the* WR *Star*

Johnson and Hogg (1965) suggested that the material ejected by the WR star sweeps up the ambient interstellar matter. While there seems no doubt that the mass loss from that star controls the shape of the nebula we would like to consider more thoroughly the probable origin of the gas in the nebula. If, as suggested by Smith (1972) all population *I* WR stars are 10 $M_\odot$ nearly pure helium stars, it follows that they have probably evolved from more massive stars from which the whole outer, hydrogen-rich envelope ($\sim$20 $M_\odot$) has been lost. When the WR star is a member of a binary system, it is probable that the material lost by the WR star has been transferred to the companion which becomes thereby fairly massive and readily detectable (Paczynski, 1967). However, when a companion is not detectable, the material must have been lost to the surrounding interstellar medium. It is notable that "ring" nebulae are associated only with WR stars that appear to be single.

We suggest that the material observed in NGC 6888 and other ring nebulae is part of the material shed by the central star in the process of becoming a WR star. The material will probably not be either uniformly distributed or at rest with respect to the star, as assumed in the dynamical models. The effect of this change is not clear. Since the origin of the shed material is the outer envelope of the star, its composition is nearly primordial. Slight *N* enrichment is possible and may contribute to the strong [N II] lines observed, but the amount of enrichment is expected to be small.

5.4. *The* [N II] *Lines*

On the assumption that the nebula was collisionally ionized and excited, Parker (1964) could explain the high values of I([N II])/(H_α) by a kinetic temperature of 15000 K. In as much as WR stars have high luminosity and probably high temperature, the radiation from the star is expected to dominate the ionization and energy balance in the nebula. The demonstration (Smith, 1968c) that WR stars are often located near the middle of such nebulae leaves no doubt regarding the real association of the star and the nebula. Thus, the relevance of Parker's analysis is uncertain (as he, himself, pointed out).

One contributor to *N*-enrichment in the nebula was suggested in Section 5.3. Another possible source is the stellar wind. This provides material highly enriched in He and N. However, in the lifetime of the nebula, $\sim 10^4$ years (Georgelin and Monnet, 1970), the stellar wind material cannot cool from the high temperature ($10^7 - 10^8$ K) produced by passage through the shock front; it remains in the hot inner shell which is unobservable.

The dominant reason for the strong [N II] lines in NGC 6888 is probably the low degree of ionization of N. N^+ has an ionization potential nearly equal to that of He. Thus, in the vicinity of hot stars it is mostly ionized to N^{++}. Two factors probably contribute to decrease ionization of N^+ in NGC 6888. Firstly, the radiation from the star is more dilute than for normal H II regions because of the shell structure. Note, that the [N II]/H_α ratio is 3 times greater at the northeast end of the nebula than at the northwest side (Parker, 1964). The distances from the star are 9 and 6 arcmin, respectively, yielding a difference in dilution factor of 2.2, approximately correct to account for the observed effect. Secondly, the high abundance of He in the atmosphere of the star is likely to depress the emergent radiation shortwards of the He ionization limit.

5.5. *The Nature of the Filaments*

Probably the most conspicuous result from our observations is the close agreement between the radio and the optical pictures. As has been shown in Section 3, the radio radiation is probably bremsstrahlung. From the observed spectrum we conclude that any non-thermal contribution at 600 MHz $<0.3\times10^{-26}$ W m^{-2} Hz^{-1}.

Mainly on descriptive grounds we distinguished in previous sections between "filaments" and the "smooth component". The question then arises whether the physical conditions in the two components differ. In Section 4.2 we showed that, to within 50%, the temperatures of the smooth component and the filaments agree. We have no direct information on the density n_e in the smooth component, but assuming that pressure equilibrium exists between the smooth component and the filaments, the densities also agree. Hence, we may conclude that there is no physical difference between smooth component and filaments: the smooth component is a "smeared" collection of filaments.

The assumption of pressure equilibrium is supported by a closer look at Pikel'ner's model (see Section 5.1). In this model the interstellar matter enters the shell through a shock front, is thereby heated and then flows away very slowly from the shock front under almost isobaric conditions. In this flow the gas cools down until its temperature is in equilibrium with the stellar UV flux. From the amount of swept up material we estimate that n_i, the density of unshocked interstellar material, equals 2 cm^{-3}. Taking the northeast corner, where the shock velocity $V=100$ km s^{-1}, we find that right after the shock $T=3\mu V^2/16k=2.7\times10^5$ K. The density is then 8 cm^{-3} and therefore $n_eT=6.4\times10^6$ K cm^{-3}. In the filaments we have $n_e=250$ to 400 cm^{-3} and $T_e=15000$ K, so that n_e T(filaments) $=3$ to 6×10^6 K cm^{-3}. The good agreement between the values of n_eT in the gas directly beyond the shock and that in the filaments supports the view that the filaments form in the shocked interstellar gas when it flows away from the shock front. Some uncertainty is introduced, however, if we assume that the outside magnetic field is fully compressed by the shock front. Taking $B=2\,\mu$G for the interstellar field, we then find that in the filaments $B^2/8\pi=6\times10^{-9}$ erg cm^{-3}, which is 5 times higher than the gas pressure $2n_ekT=1.4\times10^{-9}$ erg cm^{-3}. A suggestion as to why and how filaments may form in the cooling gas has been made by McCray *et al.* (1972). Isobarically cooling gas in the relevant temperature range is thermally unstable (Field, 1965), but the wavelengths of the resulting instabilities depend on thermal conduction. McCray *et al.* noted that the coefficient of thermal conduction is considerably smaller perpendicular to the magnetic field than parallel, and they suggest that the thermal instabilities will lead to long thin cylinders of cooler gas parallel to the magnetic field lines. To our knowledge, detailed calculations do not exist about the growth of the instability out of the linear regime.

Some support for this formation mechanism may be obtained from another case where, under different conditions, the same mechanism appears to be operating. This case is IC 443, an old supernova remnant with a well developed filamentary system. The optically observed parameters of the filaments have similar values ($n_e\approx200$–400 cm^{-3}, $V\approx65$ km s^{-1}) as in NGC 6888. The source has recently been mapped at radio wavelength with sufficient angular resolution by Duin (Duin, 1974; Duin and van der Laan, 1975). Duin shows that also in IC 443 the filamentary structure and the radio structure agree in detail. However, IC 443 is a very strong non-thermal radio source ($S=105\times10^{-26}$ W m^{-2} Hz^{-1} at 21 cm). Presumably, the synchrotron radiation is produced by interstellar cosmic ray electrons which, together with the surrounding interstellar magnetic field, have been compressed after passage through the shock front. However, the optically observed filaments do not contain enough matter to produce the radiation and Duin supposes that the optically observed filaments are actually the ionized outer edges of much more massive neutral filaments. These neutral cores contain the compressed electrons and field. The amount of hypothetical neutral matter required for this is in quantitative agreement with the amount of interstellar matter required for the slowing down of the supernova remnant.

Comparing IC 443 with NGC 6888, the striking difference is that the first is a strong non-thermal radio source, whereas the other is completely thermal. The suggestion is that IC 443 contains a large amount of neutral interstellar matter because (a) it is in a region of higher surrounding density and (b) the ejected shell was originally so energetic that it could expand to a diameter of 27 pc. NGC 6888 is situated in a region of low interstellar density, and the kinetic energy fed into the shell is considerably less. Consequently, it has swept up less matter, which will remain ionized due to the UV flux of the central star. Both effects will decrease the non-thermal radio flux.

Qualitatively, the similarities and differences between IC 443 and NGC 6888 can be understood, if we adopt the suggestion by McCray *et al.* (1972) that the magnetic field is important for the filament formation even though it may not be dynamically dominant.

5.6. HD *192163, a Radio Star?*

If a star is losing mass isotropically at a rate $\dot{M}$, with outflow velocity V_0 then the electron density distribution around the star will be given by:

$$\dot{M}=4\pi\mu\, n_e r^2 V_0$$

and, since V_0 will be constant, $n_e\sim r^{-2}$. Several authors (Panagia and Felli, 1975; Wright and Barlow, 1975; Olnon, 1975) have noticed that the bremsstrahlung flux from such an electron density distribution can be given in a closed expression, provided that the electron temperature is constant. If the mass loss is sufficiently high, the gas is optically thick and the flux density varies, in the radio region, as $\nu^{0.6}$. Such spectra have been recently observed from the small objects MWC 349 and V 1016 Cyg. Wright and Barlow show that in the infrared the spectral index is expected to increase to 2/3, provided that the line of sight through the object will reach an optical depth of 0.25 before the two conditions, $n_e \sim r^{-2}$ and T_e=constant, break down.

HD 192163 has been observed by Hackwell *et al.* (1974) at 6 wavelengths between 2.3 μ and 11.4 μ. They find considerable IR excess over that expected from extrapolation of the stellar continuum. They attribute this excess to free-free emission. At 10 μ, the flux density is 1.2×10^{-26} W m^{-2} Hz^{-1}, which predicts, for a $\nu^{0.65}$ law, S(6 cm)=4.2 10^{-29} W m^{-2} Hz^{-1}, in agreement with the uncertain detection mentioned in Section 3.3.

The corresponding value for the rate of mass loss, $\dot{M} = 2 \times 10^{-5} M_\odot$ yr^{-1} (Hackwell *et al.*, 1974), is somewhat higher than the value obtained from dynamical considerations. The latter, however, assumes spherical symmetry and constant rate of mass loss, which may be poor approximations.

Acknowledgements. As we have presented so many data it is clear that this study would not have been possible without the help of many individuals and institutions. To all of them we express our thanks: especially the Hale Observatories, Pasadena, Cal.; the Lowell Observatory Flagstaff, Ariz.; the Observatoire de Marseille and the Observatoire de Haute Provence; the NASA Goddard Space Flight Center, Green Belt, Md.; the Netherlands Foundation for Radio Astronomy; and the Max-Planck-Institut für Radioastronomie. We wish to thank Dr. R. M. Price for many helpful discussions and initiating the project.

One of us (HRD) acknowledges support from the National Science Foundation of USA.

The Westerbork Radio Observatory is operated by the Netherlands Foundation for Radio Astronomy with the financial support of the Netherlands Organization for the Advancements of Pure Research (Z.W.O.).

References

Altenhoff, W. J., Mezger, P. G., Wendker, H. J., Westerhout, G. 1961, Veröffent. Univ. Sternw. Bonn No. 59, part IV
Avedisova, V. S. 1972, *Astron. Zh.* **48**, 894, *Soviet Astron. A. J.* **15**, 708
Baars, J. W. M., Hooghoudt, B. G. 1974, *Astron. & Astrophys.* **31**, 323
Casse, J. L., Muller, C. A. 1974, *Astron. & Astrophys.* **31**, 333
Courtès, G. 1973, *Vistas Astron.* **14**, 81
Crampton, D. 1971, *Monthly Notices Roy. Astron. Soc.* **153**, 303
Dickel, H. R., Wendker, H. J., Bieritz, J. H. 1969, *Astron. & Astrophys.* **1**, 270
Duin, R. M. 1974, High resolution radio investigation of four supernova remnants. Thesis, University of Leiden
Duin, R. M., van der Laan, H. 1975 (in preparation)
Ekers, R. D., Allen, R. J., Luyten, J. R. 1973, *Astron. & Astrophys.* **27**, 77
Felli, M., Churchwell, E. 1972, *Astron. & Astrophys. Suppl.* **5**, 369
Field, G. B. 1965, *Astrophys. J.* **142**, 531
Georgelin, Y. P., Monnet, G. 1970, *Astrophys. Letters* **5**, 239
Hackwell, J. A., Gehrz, R. D., Smith, J. R. 1974, *Astrophys. J.* **192**, 383
Högbom, J. A., Brouw, W. N. 1974, *Astron. & Astrophys.* **33**, 289
Johnson, H. M. 1953, *Astrophys. J.* **118**, 370
Johnson, H. M. 1971, *Astrophys. J.* **167**, 491
Johnson, H. M., Hogg, D. E. 1965, *Astrophys. J.* **142**, 1033
Kuhi, L. V. 1966, *Astrophys. J.* **143**, 753
Lozinskaya, T. A. 1970, *Astron. Zh.* **47**, 122 = *Soviet Astron. A. J.* **14**, 98
Lozinskaya, T. A., Esipov, V. F. 1968, *Astron. Zh.* **45**, 1153 = *Soviet Astron. A. J.* **12**, 913
McCray, R., Stein, R. F., Schwarz, J. 1972, *Astrophys. J.* **177**, L 75
Olnon, F. M. 1975, *Astron. & Astrophys.* **39**, 217
Oster, L. 1961, *Rev. Mod. Phys.* **33**, 525
Paczynski, B. 1967, *Acta Astron.* **17**, 355
Panagia, N., Felli, M. 1975, *Astron. & Astrophys.* (in press)
Parker, R. A. R. 1964, *Astrophys. J.* **139**, 493
Pengelly, R. M. 1964, *Monthly Notices Roy. Astron. Soc.* **127**, 157
Pikel'ner, S. B. 1968, *Astrophys. Letters* **2**, 97
Pikel'ner, S. B., Shcheglov, P. V. 1969, *Astron. Zh.* **45**, 953; *Soviet Astron. A. J.* **12**, 757
Schwartz, R. 1968 (private communication)
Smith, L. F. 1968a, *Monthly Notices Roy. Astron. Soc.* **138**, 109
Smith, L. F. 1968b, *Monthly Notices Roy. Astron. Soc.* **140**, 409
Smith, L. F. 1968c, in *Wolf-Rayet Stars* p. 40, Eds. Gebbie, K. B., Thomas, R. N., U.S. Government Printing Office, Washington, D.C.
Smith, L. F. 1972, in *Wolf-Rayet and High Temperature Stars* p. 15, Eds. Bappu, M. K. V., Sahade, J., IAU *Symp.* No. 49
Smith, L. F., Batchelor, R. A. 1970, *Australian J. Phys.* **23**, 203
Smith, L. F., Kuhi, L. V. 1970, *Astrophys. J.* **162**, 535
Someren Grève, H. W. van 1974, *Astron. & Astrophys. Suppl.* **15**, 343
Terzian, Y. 1970, *Astron. J.* **75**, 1155
Wendker, H. J. 1970, *Astron. & Astrophys.* **4**, 378
Westerlund, B. E. 1966, *Astrophys. J.* **145**, 724
Wright, A. E., Barlow, M. J. 1975, *Monthly Notices Roy. Astron. Soc.* **170**, 41

H. J. Wendker
Hamburger Sternwarte
D-2050 Hamburg 80, Gojenbergsweg 112
Federal Republic of Germany

L. F. Smith
Max-Planck-Institut für Radioastronomie
D-5300 Bonn 1, Auf dem Hügel 69
Federal Republic of Germany

F. P. Israel
H. J. Habing
Sterrewacht, Huygens Laboratorium
Wassenaarseweg 78
Leiden-2405, The Netherlands

H. R. Dickel
University of Illinois Observatory
Urbana, Illinois 61801, USA